Oxidation of Metals, Vol. 46, Nos. 5/6, 1996

An Analysis of the Internal Oxidation of Binary M–Nb Alloys Under Low Oxygen Pressures at 600–800°C

F. Gesmundo,* Y. Niu,† F. Viani,* and F. C. Rizzo‡

Received March 5, 1995; revised March 21, 1996

The corrosion of M–Nb alloys based on iron, cobalt, and nickel and containing 15 and 30 wt% Nb has been studied at 600–800°C under low oxygen pressures (10^{-24} atm at 600°C and 10^{-20} atm at 700–800°C). Except for the Co–Nb and Ni–Nb alloys corroded at 800°C, which formed external scales of niobium oxides, corrosion under low O_2 pressures produced an internal oxidation of niobium. This attack was much faster than expected on the basis of the classical theory. Furthermore, the distribution of the internal oxide in the alloys containing two metal phases was very close to that of the Nb-rich phase in the original alloys. These kinetic, microstructural, and thermodynamic aspects are examined by taking into account the effects of the limited solubility of niobium in the various base metals and of the two-phase nature of the alloys.

KEY WORDS: niobium alloys; oxidation; high temperatures.

INTRODUCTION

The oxidation of M–Nb alloys with M = Fe, Co, and Ni and containing 15 and 30 wt% Nb has been studied at 600–800°C under low oxygen pressures (10^{-24} atm at 600°C and 10^{-20} atm at 700–800°C), obtained using H_2–CO_2 gas mixtures of appropriate compositions.[1–3] These studies were carried out

*Istituto di Chimica, Facolta' di Ingegneria, Universita' di Genova, Fiera del Mare, Pad. D, 16129 Genova, Italy.
†Corrosion Science Laboratory, Institute of Corrosion and Protection of Metals, Academia Sinica, Wencui Road 62, 110015 Shenyang, China.
‡Departmento de Ciência dos Materiais e Metalurgia, Pontificia Universidade Católica do Rio de Janeiro, Caixa Postal 38008, 22453-900, Rio de Janeiro, Brasil.

0030-770X/96/1200-0441$09.50/0

as a basis for the interpretation of the corrosion behavior of the same alloys in mixed oxidizing–sulfidizing environments produced by ternary mixtures of the H_2–H_2S–CO_2 type providing the same oxygen pressures as the H_2–CO_2 mixtures and in addition a sulfur pressure of 10^{-8} atm, which were used to simulate the atmospheres typical of coal gasification.[4–6] The experimental results concerning the measurements of corrosion of these alloys in the H_2–CO_2 mixtures have already been presented elsewhere[1–3] and thus are only briefly summarized here. The aim of the present paper is to present a unified discussion of the experimental results obtained for the three systems, with a particular regard to the special nature of these alloys and specifically to the small solubility of niobium in the base metals and to the presence of two phases in the starting materials. In particular, the Fe–Nb alloys contained a mixture of nearly pure Fe (alpha) and of an intermediate phase with a composition close to Fe_2Nb (beta).[1] The Co–Nb alloys contained a mixture of nearly pure cobalt (alpha) with an intermediate phase having a composition close to Co_3Nb (beta).[2] Finally, the Ni–Nb alloys were composed of a mixture of the two intermetallic phases Ni_8Nb (beta) and Ni_3Nb (gamma).[3] However, Ni–15Nb and Co–30Nb were nearly single-phase Ni_8Nb and Co_3Nb, respectively. Special attention is devoted to the kinetics of internal oxidation of these alloys.

SUMMARY OF THE EXPERIMENTAL RESULTS

The oxidation of binary alloys based on Fe, Co, and Ni and containing 15 and 30 wt% Nb under low oxygen pressures obtained by means of H_2–CO_2 gas mixtures at 600–800°C generally produced an internal oxidation of niobium with formation of niobium oxides (NbO_2 and/or Nb_2O_5) in a matrix of the pure metal M. In a few cases the formation of double oxides of the MNb_2O_6 type has also been observed. Moreover, in some cases, and specifically for the two Co–Nb and Ni–Nb alloys at 800°C, external oxidation of niobium was observed.[2,3] The corrosion of the two Fe–Nb alloys at 600 and 700°C, when the gas-phase oxygen pressure was above the dissociation pressure of FeO, did not lead to the growth of external scales of iron oxides, very likely as a result of a lack of equilibrium at the alloy–gas interface.[1] The internal oxidation of the two Fe–Nb alloys[1] and of the alloy Co–15Nb,[2] which contain two metal phases, produced a very fine mixture of niobium oxide and the base metal, which had the same spatial distribution as the particles of the Nb-rich phase in the original alloy. The alloys containing only a single phase (Co–30Nb and Ni–15Nb) were converted also in a fine mixture of base metal and niobium oxide, which, however, had no correlation with the microstructure of the starting materials.[2,3] Finally, oxidation of the two-phase alloy Ni–30Nb produced a mixture of Ni metal

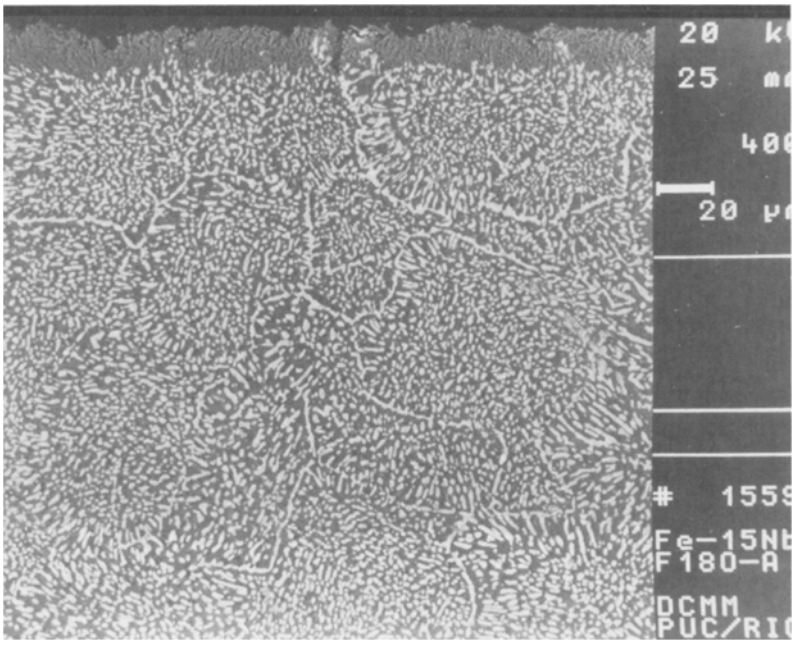

Fig. 1. Cross section (BEI) of Fe–15wt% Nb corroded at 800°C for 24 h under 10^{-20} atm O_2.

and Nb oxides for both metal phases, because also the Ni-rich phase Ni_8Nb has a rather high Nb content. Examples of the structure of samples of M–Nb alloys exposed to internal oxidation are shown in Figs. 1–4 for the three systems. A detailed description of the experimental results as well as an interpretation of the microstructures observed is given elsewhere.[1–3]

The kinetics of internal oxidation have been followed by means of continuous weight-gain measurements with the help of a microbalance. In some cases the observed rates were strictly parabolic, while in others significant deviations from the parabolic rate law were observed. Approximate values of the parabolic rate constants k_p ($g^2\,cm^{-4}\,s^{-1}$) have been calculated when possible from the weight-gain data. Moreover, experimental values of the parabolic rate constants k_x, expressed in terms of thickness of the region of internal oxidation, have been obtained from cross sections of corroded samples by measuring the final thickness of the region of internal oxidation, which was usually very evident in the corresponding BEI micrographs, using the parabolic rate law in the form

$$X^2 = k_x t$$

where X is the thickness of the internal oxidation region. The values of the rate constants relevant for the present analysis are reported below.

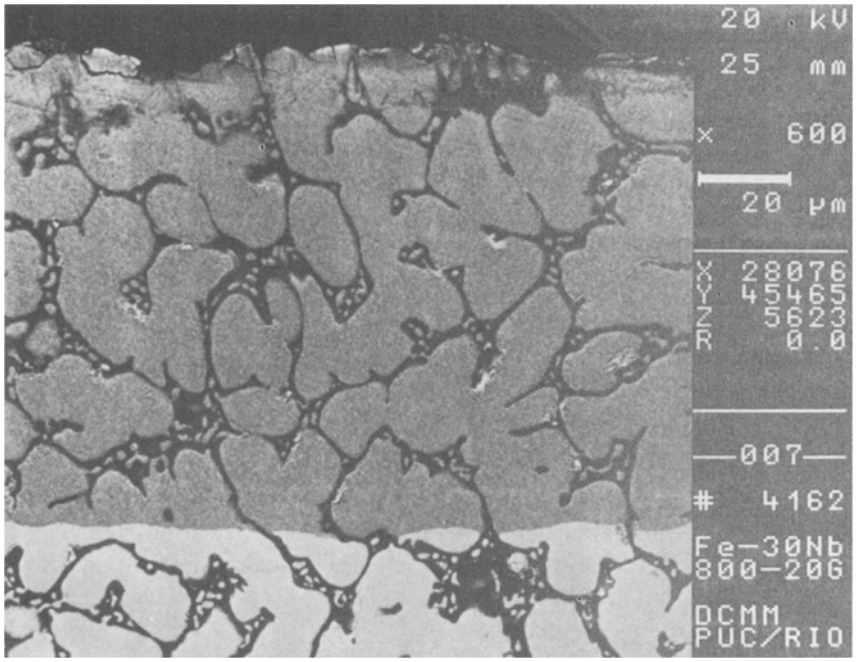

Fig. 2. Cross section (BEI) of Fe–305wt% Nb corroded at 800°C for 24 h under 10^{-20} atm O_2.

DISCUSSION

The main aspects of the oxidation of the M–Nb alloys under low oxygen pressures, including a discussion of the thermodynamic and kinetics factors involved and taking into account the microstructures of the present alloys and their relation with those of the scales produced by oxidation are examined below.

Thermodynamic Aspects

The thermodynamic predictions concerning the stability of the oxides of the various metals are reported in Figs. 5–8 by means of plots of the oxygen pressures for the equilibrium between the metals and their oxides as well for the equilibria between the various oxides, when appropriate, as functions of temperature. According to these data the oxygen pressure of 10^{-24} atm used at 600°C and of 10^{-20} atm used at 700°C are in the field of stability of Fe_3O_4, but very close to the FeO/Fe_3O_4 equilibrium. Under all the other conditions the oxygen pressures used are too low for the oxidation

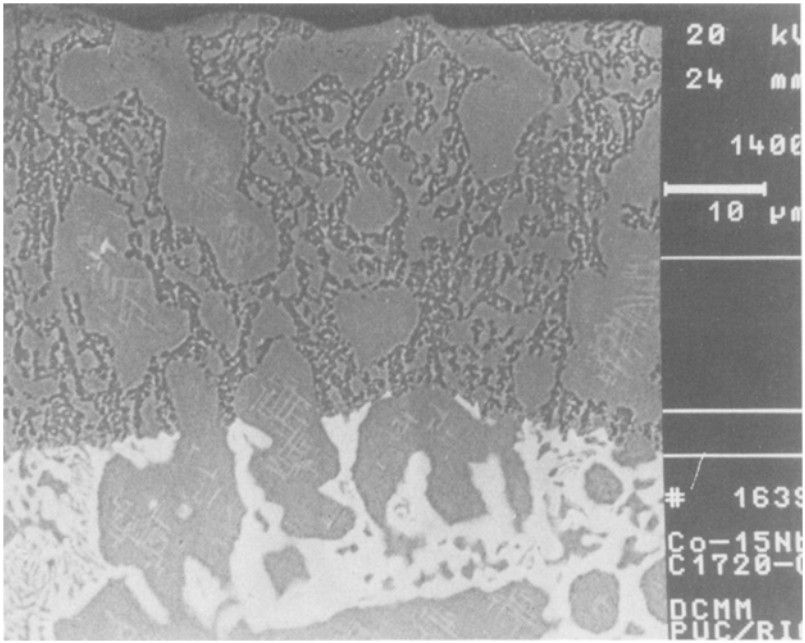

Fig. 3. Cross section (BEI) of Co–15wt% Nb corroded at 700°C for 24 h under 10^{-20} atm O_2.

of the base metals. On the contrary, these pressures are always in the field of stability of Nb_2O_5, so that in the oxidation of pure Nb all the oxides (NbO, NbO_2, and Nb_2O_5) are expected to form. However, the activity of niobium in the present alloys is very likely much smaller than unity in view not only of its relatively low average mole fraction but especially of the nonideal behavior of the alloys. In fact, for alloys forming intermetallic compounds the activity coefficients of both components are significantly smaller than unity, especially under low concentrations of the component concerned.[7]

The fields of stability of the various oxide phases for the ternary M–Nb–O systems calculated from the relevant thermodynamic data at 700°C are shown in Figs. 9–11, where they are plotted as functions of the activity of niobium. In addition to the pure oxides, the base metals and Nb are also assumed to form double oxides of the MNb_2O_6 type, which have been detected in some cases in the scales on these alloys.[1–3] The other double oxides formed by these systems[8] have been neglected for simplicity. Since the thermodynamic data concerning the stability of these ternary compounds are not known, the standard free energy of formation of the double oxides has been calculated by assuming that the standard free-energy change

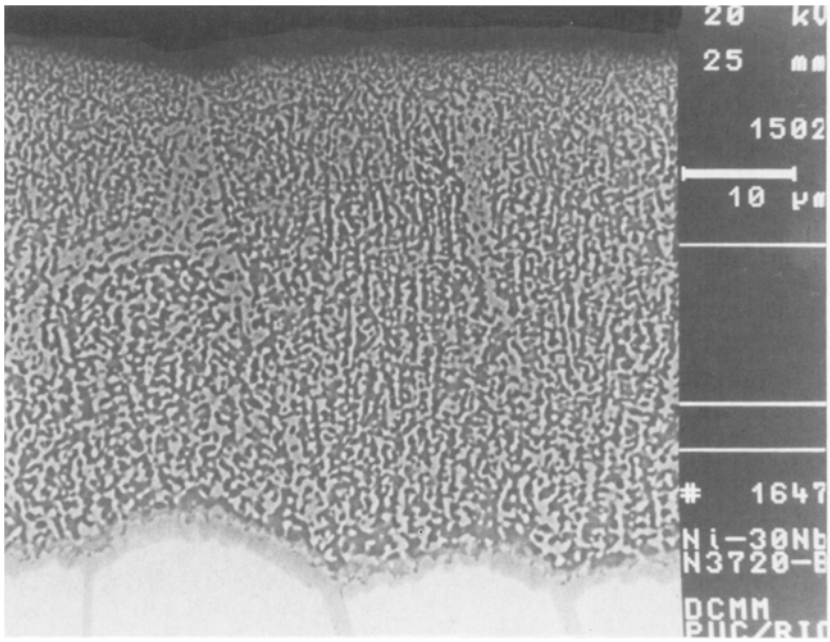

Fig. 4. Cross section (BEI) of Ni–30wt% Nb corroded at 700°C for 24 h under 10^{-20} atm O_2.

associated with the reaction between the oxides MO and Nb_2O_5 to form the double oxide, i.e.,

$$MO + Nb_2O_5 = MNb_2O_6 \qquad (a)$$

is equal to 42 kJ/mol, which is of the order of magnitude of the values reported for the formation of spinels from the corresponding pure oxides.[9]

According to these phase diagrams, the lower oxide NbO becomes unstable in contact with alloys in which the activity of Nb is lower than about 10^{-2}, which is probably higher than that prevailing in these alloys in view of the significant deviations from ideal behavior implied by the formation of intermetallic phases.[7] On the contrary, the Nb oxides NbO_2 and Nb_2O_5 should be stable in the range of Nb concentrations examined. However, the range of stability of Nb_2O_5 in terms of oxygen pressures may be significantly decreased if the oxide MO is rather stable and the free-energy change associated with reaction (a) is sufficiently large and negative because under these conditions the double M–Nb oxides become stable at quite low oxygen pressures. These considerations may explain the absence of NbO from all the systems as well as the presence of the double oxides in a limited number of cases for the Fe–Nb and Co–Nb alloys. The absence of double

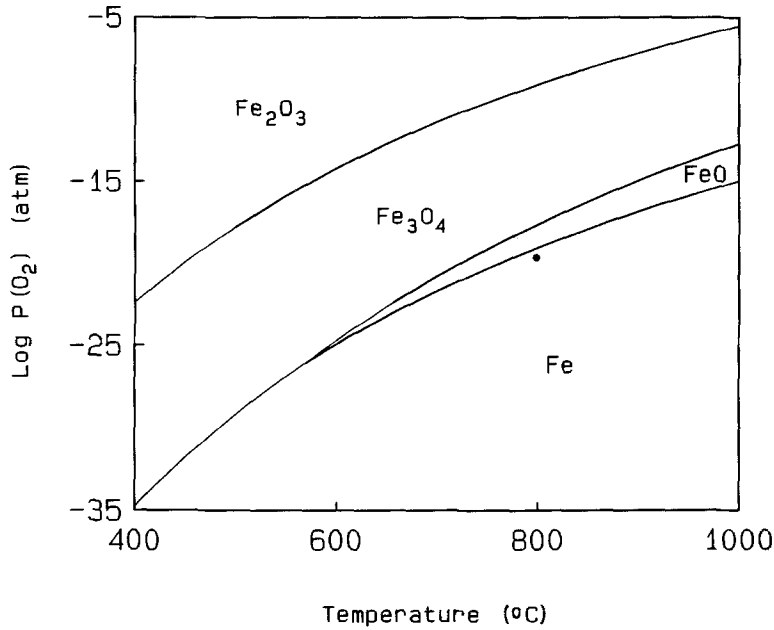

Fig. 5. Oxygen pressures for the various equilibria in the Fe–O system as functions of temperature with an indication of the values used in the present work.

oxides in the oxidation of the Ni–Nb alloys is attributed to the lower stability of NiO as compared to FeO and CoO.

A schematic phase diagram of ternary systems M–Nb–O for metals M forming with Nb intermetallic compounds and double oxides of the MNb_2O_6 type is shown in Fig. 12. The M-rich side contains three metal phases, i.e., a solid solution of Nb in M (alpha) and two intermetallic compounds of formula M_3Nb (beta) and MNb (gamma), while the Nb-rich side has not been developed in detail. In spite of the low solubility of Nb in the base metals, and particularly in Fe and Co, the alloy composition for the simultaneous equilibrium with the base-metal oxide MO and the double oxide has been selected in the field of stability of the alpha phase under the oxygen pressure P_1, in view of the rather large difference between the thermodynamic stabilities of the oxides of the base metals and of Nb. Furthermore, the oxygen pressure for the equilibrium between the alloy, the double oxide, and Nb_2O_5 has also been located in the field of stability of the alpha phase under the oxygen pressure P_3. The oxygen pressures for the alpha-beta-Nb_2O_5 and the beta-gamma-Nb_2O_5 equilibria are denoted as P_4 and P_5, respectively. Finally, the pressure for the equilibrium between pure M and MO is equal to P_2, while that prevailing in the gas phase is equal to P^g. In

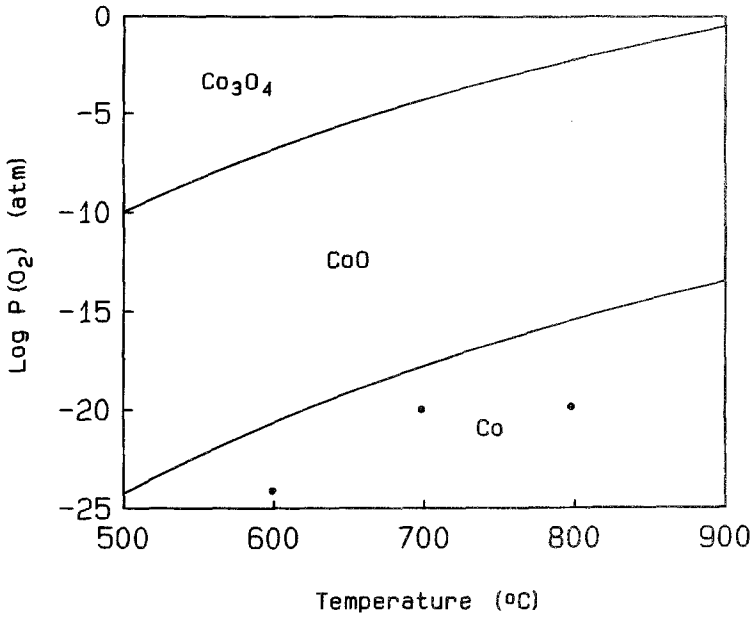

Fig. 6. Oxygen pressures for the various equilibria in the Co–O system as functions of temperature with an indication of the values used in the present work.

addition, Nb_2O_5 has been considered stable in the whole pressure range between P_5 and P_3.

Structure of the Scales

For the Fe–Nb and Co–Nb alloys which contain a mixture of the solid solution of Nb in the base metal and an intermetallic compound (Fe_2Nb and Co_3Nb, respectively), the internal oxidation regards essentially only the beta phase, because the concentration of Nb dissolved in the alpha phase is very low.[10] For these systems the distribution of the particles of internal oxide follows closely that of the alloy islands rich in niobium. On the contrary, the two Ni–Nb alloys contain a mixture of the two phases Ni_8Nb (beta) and Ni_3Nb (gamma), both of which are transformed into a mixture of base metal and niobium oxide, because also the beta phase contains a significant concentration of niobium. Moreover, in most cases these alloys do not develop a Nb-depleted layer at the interface with the zone of internal oxidation.

The internal oxidation of these alloys is different from that typical of single-phase alloys, as described by the theory developed by Wagner[11]

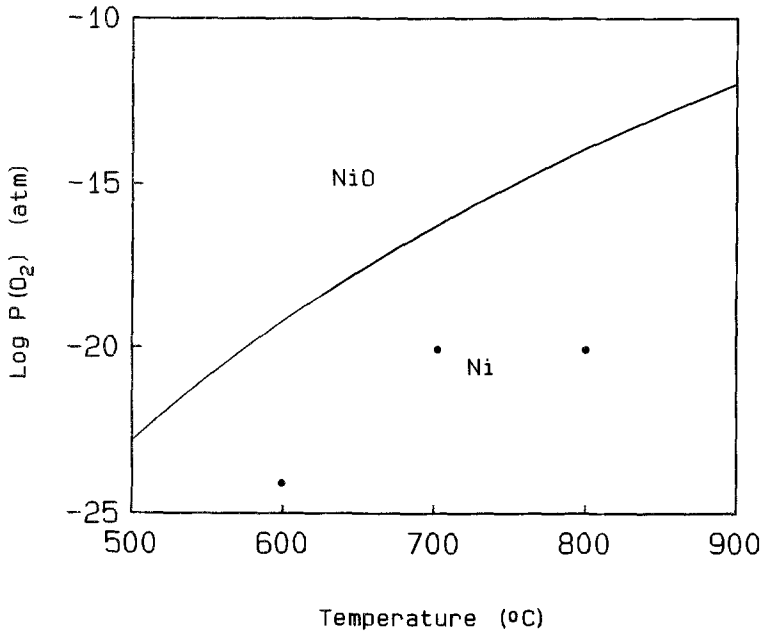

Fig. 7. Oxygen pressures for the various equilibria in the Ni–O system as functions of temperature with an indication of the values used in the present work.

and summarized later by Rapp.[12] In fact, the classical type of internal oxidation leads to a uniform distribution of the oxide particles in the base-metal matrix, reflecting that of the same component in the alloy. On the contrary, the internal oxidation of the present alloys does not involve any important diffusion of the most-reactive component B (Nb). This behavior has been predicted recently for the internal oxidation of two-phase binary A–B alloys in which B has a small solubility in the base metal A and a small diffusivity in A compared to that of oxygen.[13–15] Under these conditions, oxygen penetrates through A and reacts with B locally, forming the corresponding oxide(s) without involving any significant metallic diffusion. This form of corrosion, which has been denoted "diffusionless" or *in situ* internal oxidation,[13–15] produces a peculiar distribution of the particles of internal oxide which follows closely that of the particles rich in B in the alloy.[13–15]

With reference to Fig. 12, the structure of the regions of internal oxidation corresponds to a diffusion path running vertically in the plot from the oxygen pressure P_4 up to the oxygen pressure prevailing at the alloy–gas interface (dashed line). Thus, under an oxygen pressure equal to P_4 the beta phase will start to decompose into a mixture of nearly pure M and niobium

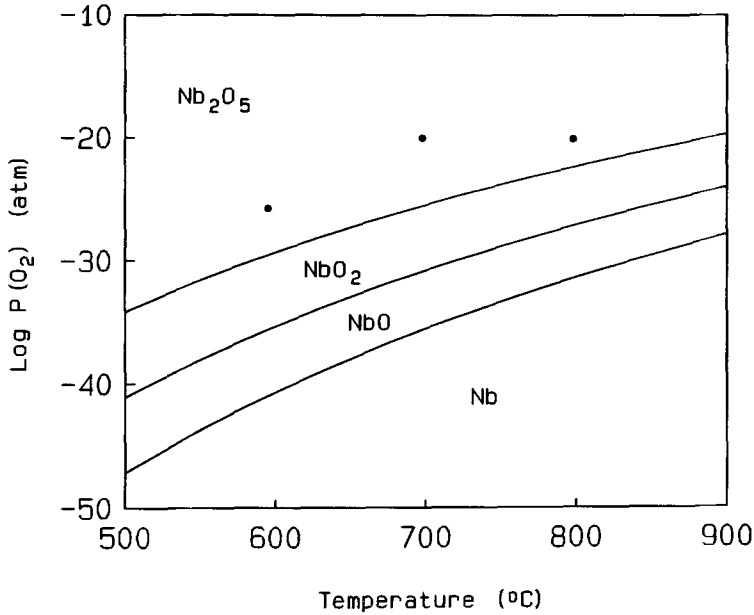

Fig. 8. Oxygen pressures for the various equilibria in the Nb–O system as functions of temperature with an indication of the values used in the present work.

oxide, which will remain stable up to an oxygen pressure equal to P_3, while in the range between P_3 and P_g the alloy will be in equilibrium with the double oxide. Furthermore, in agreement with this analysis, the two-phase alloys do not develop a region of Nb depletion beneath the internal-oxidation front.[1-3]

Another important difference between the internal oxidation of two-phase and single-phase alloys regards the condition for the transition from the internal to the external oxidation of B in the absence of an external scale of the oxide of the base metal A. For single-phase alloys this requires that the volume fraction of internal oxide exceeds a critical value which has been found equal to 0.3 for Ag–In alloys.[16] For two-phase alloys if the solubility of B in A is too low, this transition may occur only in the presence of a matrix of the B-rich phase, and thus under very high average concentrations of B.[14,15] If the solubility of B in A is not too low, the preferential consumption of B may lead to the appearance of a single-phase layer of alpha on top of the two-phase alloy. This structure may result in the external oxidation of B, but the critical average concentration of B in the alloy required for the transition for two-phase alloys is larger than for single-phase alloys under the same values of the relevant parameters.[15]

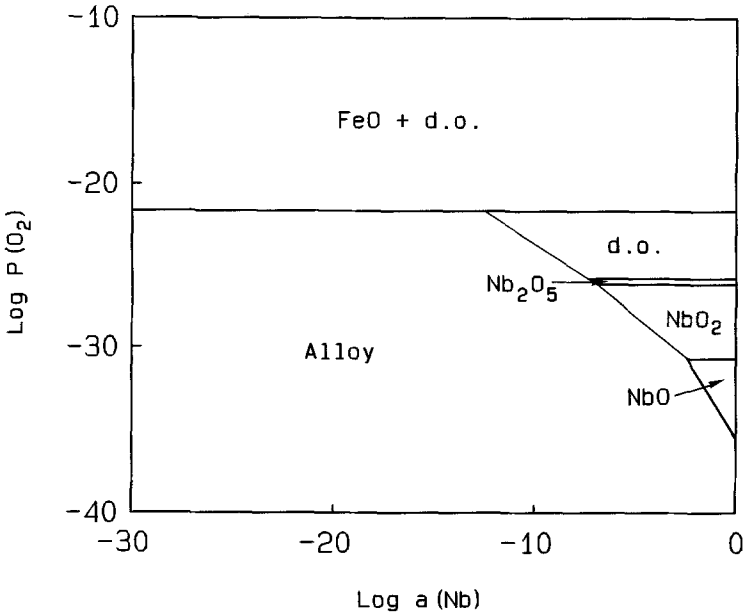

Fig. 9. Fields of stability of the various oxide phases in equilibrium with the alloy in the ternary Fe–Nb–O system at 700°C as functions of the activity of niobium in the alloy (d.o. = double-oxide $FeNb_2O_6$).

The volume fraction of internal oxide in these alloys calculated for the formation of NbO_2 and in the absence of Nb enrichment according to the equation reported below is equal to 0.21 and 0.40 for Fe–15Nb and Fe–30Nb, respectively, and to 0.23 for Co–15Nb and Ni–15Nb and 0.42 for Co–30Nb and Ni–30Nb. Thus, the values for the M–30Nb alloys are much higher than the critical value reported for single-phase alloys.[16] However, under most conditions the present alloys undergo only internal oxidation of Nb of the *in situ* type, without any significant depletion of Nb in the alloy, in agreement with previous conclusions. The external oxidation of Nb is observed only at 800°C for the two Co–Nb and Ni–Nb alloys.[2,3] This transition is a result of an increase in the diffusivity of Nb through the base metals with temperature, which allows the critical volume fraction of internal oxide to be exceeded.

Kinetics of Internal Oxidation

In priciple, the parabolic rate constants of internal oxidation for these systems may be calculated using the classical approach developed by Wagner,[11,12] assuming that the internal oxidation involves only the inward

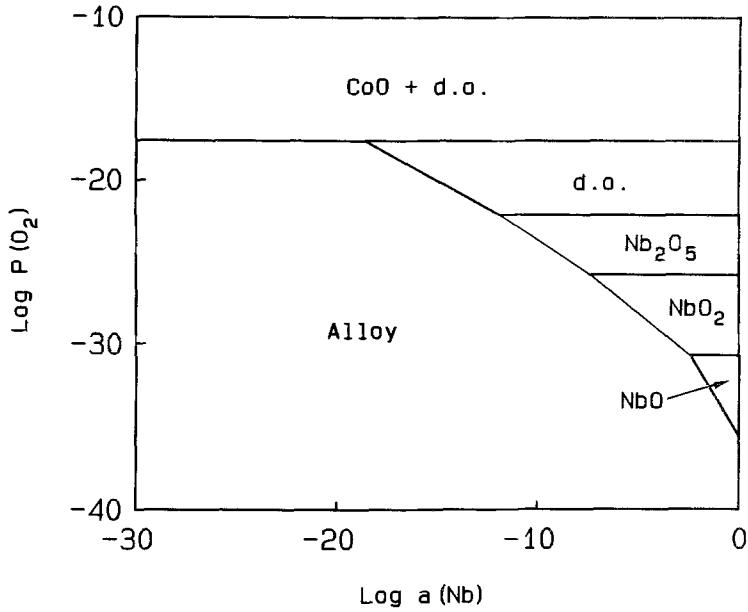

Fig. 10. Fields of stability of the various oxide phases in equilibrium with the alloy in the ternary Co–Nb–O system at 700°C as functions of the activity of niobium in the alloy (d.o. = double-oxide $CoNb_2O_6$).

penetration of oxygen by diffusion through the base metal A, while B remains immobile. The flux of oxygen at the front of internal oxidation, at a distance X from the alloy surface, $J_O(X)$, has the form[17]

$$J_O(X) = \frac{N_O^s c}{\pi^{1/2} \exp(\gamma^2) \operatorname{erf}(\gamma)} \left(\frac{D_O}{t}\right)^{1/2} \tag{1a}$$

where N_O^s, D_O, and c are the mole fraction of oxygen dissolved in A under the gas-phase pressure, the diffusion coefficient of oxygen in A, and the overall concentration of metal (A + B) in the alloy (moles/cm^3), while γ is an appropriate kinetics parameter as defined by Wagner.[11,12] Equation (1a) is the normal expression of $J_O(X)$ for the internal oxidation of single-phase binary alloys. In order to take into account the restriction to the oxygen flux due to the decrease of the cross section for oxygen diffusion produced by the internal oxide, the previous expression is modified by introducing the factor $1 - f_v$, where f_v is the volume fraction of internal oxide, obtaining

$$J_O(X) = \frac{N_O^s c(1 - f_V)}{\pi^{1/2} \exp(\gamma^2) \operatorname{erf}(\gamma)} \left(\frac{D_O}{t}\right)^{1/2} \tag{1b}$$

The difference between the oxygen fluxes given by Eqs. (1a) and (1b) may become significant when f_v becomes large.

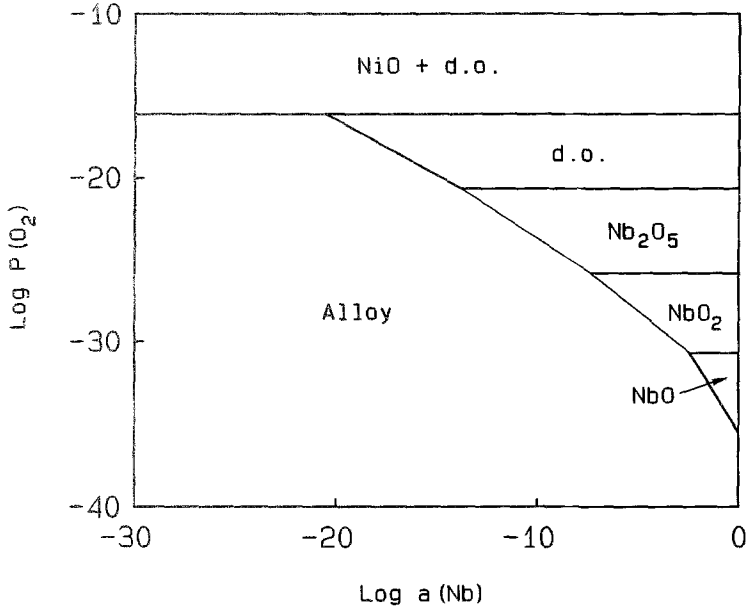

Fig. 11. Fields of stability of the various oxide phases in equilibrium with the alloy in the ternary Ni–Nb–O system at 700°C as functions of the activity of niobium in the alloy (d.o. = double-oxide $NiNb_2O_6$).

The volume fraction of internal oxide f_v may be calculated easily from the alloy composition according to the expression[14]

$$f_v = N_{ox}/[r - N_{ox}(r-1)] \tag{2}$$

where r is equal to V_{all}/V_{ox} and V_{all}, V_{ox} are the molar volumes of the alloy and of the Nb oxide, respectively, while N_{ox} is the mole fraction of internal oxide. In turn, the value of N_{ox} in the region of internal oxidation where the beta phase decomposes into the alpha phase and BO_v can be calculated from the equation

$$N_{ox} = 1 - [1 - N_B^{av}]/[1 - N_{B(\alpha)}^{s}] \tag{3}$$

where N_B^{av} is the average mole fraction of B in the original two-phase alloy and $N_{B(\alpha)}^{s}$ the solubility of B in the alpha phase.

If B does not diffuse significantly in the alloy, the number of moles of B converted into oxide during the displacement of the internal-oxidation front in a sample of surface area S in a time interval dt, dn(B), is equal to the number of moles of B contained in an alloy layer of thickness dX, where dX is equal to the advancement of the internal-oxidation front in a time

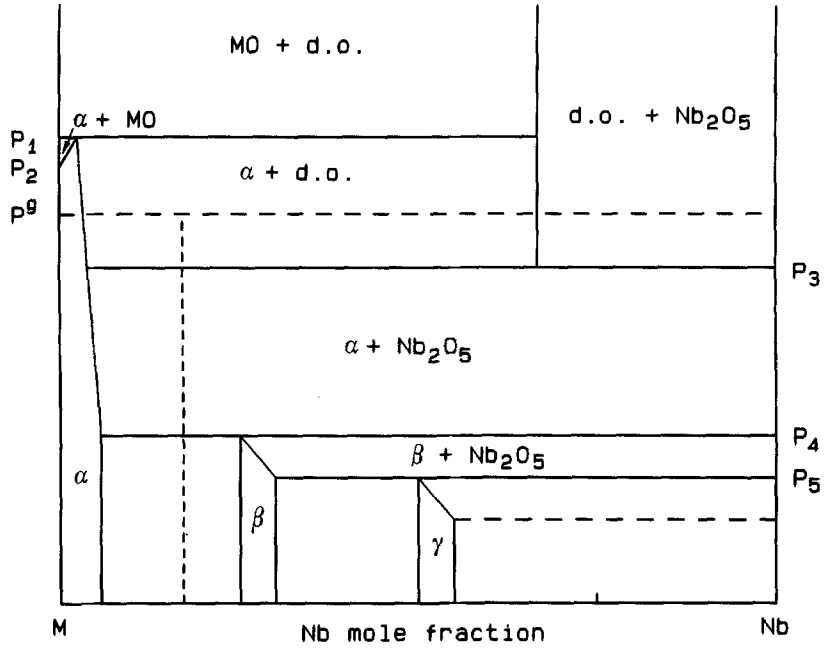

Fig. 12. Schematic isothermal phase diagram for ternary M–Nb–O systems for metals with a small solubility of niobium and forming two intermetallic compounds M_3Nb and MNb and a double oxide MNb_2O_6 with an indication of the diffusion path corresponding to the experimental results (dashed line).

interval dt. Thus, $dn(\mathrm{B})$ has the form

$$dn(\mathrm{B}) = ScN_{\mathrm{B}}^{\mathrm{av}}\, dX \tag{4}$$

If internal oxidation proceeds according to a parabolic rate law in the classical form

$$X^2 = 4\gamma^2 D_{\mathrm{O}}\, t = k_x t \tag{5}$$

one also has

$$dX = \tfrac{1}{2}(k_x/t)^{1/2}\, dt \tag{6}$$

Upon introduction of Eq. (6) into Eq. (4), one obtains

$$\frac{1}{S}\, dn(\mathrm{B}) = c\left(\frac{N_{\mathrm{B}}^{\mathrm{av}}}{2}\right)\left(\frac{k_x}{t}\right)^{1/2} dt = J_B(X)\, dt \tag{7}$$

with

$$J_B(X)=\frac{cN_B^{av}}{2}\left(\frac{k_x}{t}\right)^{1/2}=cN_B^{av}\gamma\left(\frac{D_O}{t}\right)^{1/2} \tag{8}$$

where $J_B(X)$ represents the number of moles of B transformed into oxide per unit surface area and unit time. Finally, the fluxes of O and B at $x=X$ are correlated by means of the stoichiometric condition[12]

$$J_O(X)=vJ_B(X) \tag{9}$$

where v is the oxygen/metal ratio of the internal oxide. The previous condition applies only if it is assumed that all B present in the alloy is oxidized instantaneously during the movement of the front of internal oxidation. Otherwise, v will be an empirical parameter reflecting the actual average ratio O/B for the oxidation of B at the front of internal oxidation. Using Eqs. (1a) and (8) to express the fluxes of O and B yields then

$$\frac{N_O^s}{vN_B^{av}}=G(r) \tag{10a}$$

where $G(r)$ is the auxiliary function normally used in diffusion problems, defined as[18]

$$G(r)=\pi^{1/2}r\exp(r^2)\operatorname{erf}(r)$$

If the hindering effect of the internal oxide over the O flux is taken into account, one obtains instead

$$\frac{N_O^s(1-f_v)}{vN_B^{av}}=G(r) \tag{10b}$$

Thus, knowledge of N_O^s, v, N_B^{av}, and f_v allows us to calculate γ from Eq. (10a) or (10b) and then also the rate constant k_x according to Eq. (5) if D_O is known.

The kinetics of internal oxidation may also be followed by means of weight-gain measurements. If the depth of internal oxidation follows the parabolic rate law, as normally observed, then also the weight gain per unit surface area, $\Delta M/S$, will follow the same law. Thus, the rate constant k_p defined by means of the equation

$$(\Delta M/S)^2=k_pt \tag{11}$$

is related to k_x as defined above by[19]

$$k_p=k_x(vcN_B^{av}M_O)^2 \tag{12}$$

Table I. Experimental Data for Internal Oxidation of the Fe–Nb Alloys (k_x in $cm^2\ s^{-1}$ and k_p in $g^2\ cm^{-4}\ s^{-1}$)

	i.o. depth[a]	k_x	k_p	k_x/k_p
1. At 700°C				
Fe–15Nb	51.8	3.1×10^{-10}	9.6×10^{-12}	32.3
Fe–30Nb	17.9	3.7×10^{-11}	1.6×10^{-12}	23.1
2. At 800°C				
Fe–15Nb	206.3	4.9×10^{-9}	1.0×10^{-10}	49.0
Fe–30Nb	97.4	1.1×10^{-9}	1.2×10^{-10}	9.2

[a]Overall depth of i.o. (microns) after 24-h corrosion.

where M_O is the atomic weight of oxygen. Equation (12) is different from the relation between k_x and k_p, which applies to the growth of external scales, as discussed in more detail elsewhere.[19] Equations (5) and (10) and/or Eq. (12) can be used alternatively or together to check the agreement between the calculated and experimental values of the rate constants for internal oxidation of the present alloys.

Analysis of the Experimental Data for the Kinetics of Internal Oxidation

Fe–Nb Alloys

The parabolic rate constants k_x and k_p measured experimentally for the two Fe–Nb alloys at 700 and 800°C and their ratio are reported in Table I.

The solubility and diffusivity of oxygen in alpha-iron at high temperatures have been obtained from a study of internal oxidation in Fe–Al alloys and are given by[20]

$$N_O^s = 0.381 \exp(-104/RT)\ \text{kJ/mol}$$

and

$$D_O(\text{cm}^2\ \text{s}^{-1}) = 1.79 \times 10^{-3} \exp(-85.7/RT)\ \text{kJ/mol}$$

respectively, where N_O^s refers to the oxygen pressure for the Fe–FeO equilibrium. Use of these values and of the average mole fraction of niobium in the two alloys (0.096 for Fe–15Nb and 0.205 for Fe–30Nb) and of Eqs. (10a) and (12) yields values of k_x and k_p at 800°C which are reported in Table II. For simplicity, these results concern only the formation of a single oxide of niobium, i.e., NbO_2, which is the most important in these systems.[1–3] The results of the same calculation carried out using Eq. (10b) and thus including the hindering effect of the internal oxide on the oxygen diffusion are reported again in Table II. The experimental values of both k_x and k_p are much larger than those calculated according to the present method. In particular, those calculated by means of Eq. (10a) are larger than those

Table II. Comparison Between Experimental and Calculated Values of Parabolic Rate Constants for Internal Oxidation of Fe–Nb Alloys at 800°C with Formation of NbO_2 (k_x in $cm^2\ s^{-1}$ and k_p in $g^2\ cm^{-4}\ s^{-1}$)

	k_x^c	k_p^c	k_x^c/k_p^c	k_x^e/k_p^e
Fe–15Nb	$1.3 \times 10^{-12\,a}$	$2.1 \times 10^{-13\,a}$	6.2^a	49.0
	$1.0 \times 10^{-12\,b}$	$1.7 \times 10^{-13\,b}$	5.9^b	
Fe–30Nb	$6.0 \times 10^{-13\,a}$	$4.1 \times 10^{-13\,a}$	1.5	9.2
	$3.6 \times 10^{-13\,b}$	$2.5 \times 10^{-13\,b}$	1.4	

[a] Neglecting the hindering effect of the internal oxide.
[b] Including the hindering effect of the internal oxide.

obtained from Eq. (10b), and thus closer to those measured experimentally, even if still much lower.

According to Eq. (12), the theoretical ratio k_x/k_p for a given alloy depends on the nature of the internal oxide: for the formation of NbO_2 this ratio becomes equal to 6.0 for Fe–15Nb and to 1.5 for Fe–30Nb at 800°C. The corresponding values for the formation of NbO and Nb_2O_5 are equal to 23.9 and 3.8 for Fe–15Nb and to 5.9 and 0.9 for Fe–30Nb, respectively. The experimental ratios k_x/k_p, reported also in Table II, are much higher than those predicted not only for the formation of NbO_2, but also of NbO and thus, according to Eq. (12), correspond to v values smaller than 1.

The experimental values of k_x and k_p may be used in connection with the previous treatment, developed for an ideal case, to calculate the corresponding "experimental" values of v and D_O, v^e and D_O^{eff}, respectively, which will differ from the correct values relevant to the system if k_x and k_p differ from their theoretical values. The procedure used for the calculation of v^e and D_O^{eff} is the following. Use of the ratio between the experimental values of k_x and k_p in Eq. (12) allows us to calculate the corresponding "experimental" value of v, v^e. Introduction of v^e in Eq. (10a) or (10b) with the relevant values of N_O^s and N_B^{av} yields an "experimental" value of γ, γ^e. Finally, introduction of γ^e in Eq. (5) allows us to calculate the "experimental" value of D_O, D_O^{eff}. In any case, for a given system there is only one possible combination of values of v and D_O which allows us to obtain the experimental values of both k_x and k_p.

In particular, for the present system the agreement between calculated and experimental values for both k_x and k_p may be improved by increasing the diffusion coefficient of oxygen, using an effective diffusion coefficient D_O^{eff} defined by means of an enhancement factor $E = D_O^{eff}/D_O$. Furthermore, the stoichiometric coefficient v must be decreased significantly below 2 in order to produce the experimental value of the k_x/k_p ratio. The v^e and E values which lead to a good agreement between calculated and experimental values for both k_x and k_p are reported in Table III.

Table III. Empirical Values of the Stoichiometric Coefficient v in NbO_v and of the Enhancement Factor for O Diffusion E Leading to Agreement Between Calculated and Experimental Values of k_x and k_p for Oxidation of Fe–Nb Alloys at 800°C Under 10^{-20} atm O_2

	v	E_1^a	E_2^b
Fe–15Nb	0.7	1335	1591
Fe–30Nb	0.8	733	1068

[a] Neglecting the hindering effect of the internal oxide.
[b] Including the hindering effect of the internal oxide.

Co–Nb Alloys

The diffusion coefficient of oxygen in cobalt has been evaluated from the results of internal oxidation in Co–Si alloys[21] and is given by

$$D_O(\text{cm}^2\,\text{s}^{-1}) = 67.8 \exp(-241/RT)\ \text{kJ/mol}$$

The solubility of oxygen in cobalt at high temperatures has been measured by Seybolt and Mathewson[22] and is given by

$$N_O^s = 3.28 \times 10^{-2} \exp(-36.54/RT)\ \text{kJ/mol}$$

Calculations similar to those presented above for the Fe–Nb alloys have been carried out also for the Co–Nb alloys for a temperature of 700°C, because at 800°C these alloys tend to produce an external oxidation of niobium.[2] The experimental values of the rate constants for the internal oxidation of the Co–Nb alloys at 700°C are reported in Table IV. Using the solubility and diffusivity for oxygen in cobalt reported above, the average mole fraction of niobium in the two alloys (0.100 for Co–15Nb and 0.213 for Co–30Nb), assuming the formation of NbO_2 only and using Eqs. (10a) and (12) yields the values of k_x and k_p reported in Table V at 700°C, both including or not the hindering effect of the NbO_2 particles on the diffusion of oxygen. Again, the calculated values of k_x and k_p are much lower than the corresponding experimental values, while the ratios k_x/k_p obtained from the calculated rate constants are much lower than those measured experimentally. The values of v^e and E which allow us to obtain the experimental values of the rate constants k_x and k_p for the two alloys are reported in

Table IV. Experimental Data for Internal Oxidation of Co–Nb Alloys at 700°C

	i.o. depth[a]	k_x	k_p	k_x/k_p
Co–15Nb	10	1.2×10^{-11}	2.8×10^{-13}	42.8
Co–30Nb	4	1.8×10^{-12}	1.3×10^{-13}	13.8

[a] Overall depth of i.o. (microns) after 24-h corrosion.

Table V. Comparison Between Experimental and Calculated Values of Parabolic Rate Constants for Internal Oxidation of the Co–Nb Alloys at 700°C with Formation of NbO_2 (k_x in $cm^2\ s^{-1}$ and k_p in $g^2\ cm^{-4}\ s^{-1}$)

	k_x^c	k_p^c	k_x^c/k_p^c	k_x^e/k_p^e
Co–15Nb	$4.1 \times 10^{-14\,a}$	$8.6 \times 10^{-15\,a}$	4.8^a	41.4
	$3.1 \times 10^{-14\,b}$	$6.6 \times 10^{-15\,b}$	4.7^b	
Co–30Nb	$1.9 \times 10^{-14\,a}$	$1.6 \times 10^{-14\,a}$	1.2^a	13.8
	$1.1 \times 10^{-14\,b}$	$9.2 \times 10^{-15\,b}$	1.2^b	

[a] Neglecting the hindering effect of the internal oxide.
[b] Including the hindering effect of the internal oxide.

Table VI. As in the previous case, an agreement with the experimental values of both k_x and k_p is only obtained using v^e values smaller than unity and E values larger than unity, even though significantly smaller than for the Fe–Nb alloys.

Ni–Nb Alloys

The solubility of oxygen in Ni at the Ni–NiO equilibrium is given by[23]

$$N_O^s = 8.3 \times 10^{-2} \exp(-55/RT)\ \text{kJ/mol}$$

while the diffusion coefficient of oxygen in nickel is given by[23]

$$D_O(\text{cm}^2\ \text{s}^{-1}) = 4.9 \times 10^{-2} \exp(-164/RT)\ \text{kJ/mol}$$

Calculations similar to those developed above for the Fe–Nb and Co–Nb alloys have been carried out also for the two Ni–Nb alloys for a temperature of 700°C, because at 800°C also the Ni–Nb alloys tend to produce an external oxidation of niobium.[3] The experimental values of the rate constants for the internal oxidation of the Ni–Nb alloys at 700°C are reported in Table

Table VI. Empirical Values of the Stoichiometric Coefficient v in NbO_v and of the Enhancement Factor for O Diffusion E Leading to an Agreement Between Calculated and Experimental Values of k_x and k_p for Oxidation of Co–Nb Alloys at 700°C Under 10^{-20} atm O_2

	v	E_1^a	E_2^b
Co–15Nb	0.7	97	117
Co–30Nb	0.6	28	42

[a] Neglecting the hindering effect of the internal oxide.
[b] Including the hindering effect of the internal oxide.

Table VII. Experimental Data for Internal Oxidation of Ni–Nb Alloys at 700°C

	i.o. depth[a]	k_x	k_p	k_x/k_p
Ni–15Nb	4.7	2.6×10^{-12}[b]	4.0×10^{-13}[b]	6.5
Ni–30Nb	13	2.0×10^{-11}	1.0×10^{-12}	20.0

[a] Overall depth of i.o. (microns) after 24-h corrosion.
[b] Average values.

VII. The oxidation of Ni–15Nb at 700°C does not follow the parabolic rate law to a good approximation: thus, an average value of the rate constants k_p and k_x has been used.[3] Using the solubility and diffusivity values for oxygen in nickel reported above, the average mole fraction of niobium in the two alloys (0.100 for Ni–15Nb abd 0.213 for Ni–30Nb), assuming the formation of NbO_2 only and using Eqs. (10a) and (12) yields the values of k_x and k_p reported in Table VIII at 700°C, both including or not the hindering effect of the NbO_2 particles on the diffusion of oxygen. As in the previous cases, the calculated values of k_x and k_p are much lower than the corresponding experimental values, while the ratios k_x/k_p obtained from the calculated rate constants are lower than those measured experimentally, especially for Ni–30Nb.

The values of v^e and E which allow one to obtain the experimental values of the rate constants k_x and k_p for the two alloys are reported in Table IX. As in the previous cases, an agreement with the experimental values of both k_x and k_p is only obtained using v^e values smaller than 2 and E values much larger than unity. In particular, the v^e value for Ni–15Nb is higher than unity, but in any case smaller than 2, as in the other cases. However, the E values for both alloys are again very large, and that for Ni–30Nb even much larger than for the Fe–Nb alloys.

Table VIII. Comparison Between Experimental and Calculated Values of Parabolic Rate Constants for Internal Oxidation of the Ni–Nb Alloys at 700°C (with formation of NbO_2 and neglecting the hindering effect of internal oxide) (k_x in $cm^2\ s^{-1}$ and k_p in $g^2\ cm^{-4}\ s^{-1}$)

	k_x^c	k_p^c	k_x^c/k_p^c	k_x^e/k_p^e
Ni–15Nb	8.1×10^{-16}[a]	1.7×10^{-16}[a]	4.8[a]	6.5
	6.6×10^{-16}[b]	1.4×10^{-16}[b]	4.7[b]	
Ni–30Nb	3.8×10^{-16}[a]	3.1×10^{-16}[a]	1.2[a]	20.0
	2.3×10^{-16}[b]	1.9×10^{-16}[b]	1.2[b]	

[a] Neglecting the hindering effect of the internal oxide.
[b] Including the hindering effect of the internal oxide.

Table IX. Empirical Values of the Stoichiometric Coefficient v in NbO_v and of the Enhancement Factor for O Diffusion E Leading to Agreement Between Calculated and Experimental Values of k_x and k_p for Oxidation of Ni–Nb Alloys at 700°C Under 10^{-20} atm O_2

	v	E_1[a]	E_2[b]
Ni–15Nb	1.7	2754	3202
Ni–30Nb	0.5	12727	18667

[a] Neglecting the hindering effect of the internal oxide.
[b] Including the hindering effect of the internal oxide.

Interpretation of the Kinetics of Internal Oxidation

The previous results concerning the kinetics of internal oxidation of the M–Nb alloys under low oxygen pressures are quite anomalous. An increase of the rate constant for internal oxidation with respect to the classical treatment developed by Wagner,[11,12] similar to those reported here, has already been reported for various systems, such as for the oxidation of Ni–Al[24] and Fe–Al[25] alloys and for the sulfidation of Fe–Al alloys[26] for which internal attack produced particles in the form of rods or platelets rather than of isolated spherical particles. The enhancement in the rate of internal attack in these cases has been attributed to the faster penetration of the oxidant by migration along the metal–oxide interface rather than through the bulk alloy.[24,27] The same effect, which has been found to increase with the concentration of the reactive element,[24–26] is probably operating also in the internal oxidation of the present alloys. However, the enhancement factor for the oxidant diffusion coefficient observed here for the Fe–Nb and Ni–Nb alloys is significantly larger than those observed previously,[24–26] probably as a result of the formation of a large number of very small but well interconnected oxide particles. A further important contribution to this effect may also come from the accumulation of large mechanical stresses in the alloy due to large volume increases associated with internal oxidation, in view of the large niobium content and of the high ratio between the molar volumes of the internal oxide and the alloy. These stresses produce large densities of dislocations, which are very effective preferential paths for diffusion of the various species.[28] The production of dislocations in the metal matrix as a result of the compressive stresses due to internal oxidation has been established for Ag–In alloys, where stress relief was achieved by means of transport of silver to the alloy surface.[29]

Concerning the anomalous values of v, recall that this behavior has already been observed in the oxidation of dilute alloys for some systems

containing metals presenting a large affinity for oxygen, such as dilute Ag alloys containing Al or Mg.[30–32] The average oxygen–metal ratio in these systems was above the stoichiometric value as a result of the formation of M–O clusters containing an excess of oxygen. Recently, a careful study of the internal oxidation of Ag–Mg alloys has shown that they form an outer layer containing an oxygen excess and an inner layer where substoichiometric species are present.[33] However, the situation with the present two-phase alloys is very likely a consequence of their peculiar structure and in particular of the nonhomogeneous distribution of niobium in the alloy, at variance with single-phase alloys. Thus, the low values of v^e for the present alloys are attributed to the fact that at the front of internal oxidation niobium is only partly oxidized, probably starting at the outer surface of the Nb-rich metal particles, while its complete conversion into oxide occurs only gradually with time. In this way, the penetration of oxygen becomes much faster than in the case of complete instantaneous oxidation of the Nb-rich particles, because the kinetics behavior corresponds to alloys with an overall Nb content much lower than their actual values. At the same time, the effective oxygen–niobium ratio at the front of internal oxidation involved in Eqs. (9) and (12) becomes much smaller than that required by the oxide stoichiometry, because in this case it regards only part of the metal present in the alloy.

CONCLUSIONS

The oxidation under low oxygen pressures of binary alloys formed by Fe, Co, and Ni with Nb containing 15 and 30 wt% Nb, all of which have a low solubility of Nb in the base metal and contain intermetallic phases, produces generally only a region of internal oxidation. The spatial distribution of the internal oxide reflects that of the Nb-rich phases in the starting materials and corresponds to the absence of important diffusion of niobium in the alloy. The kinetics of internal attack are not in agreement with the classical treatment of this process as a result of the partial oxidation of niobium during the advancement of the front of internal attack and of a strongly enhanced diffusion of oxygen very likely due to the presence of large oxide–metal interfaces as well as of large mechanical stresses associated with an important volume increase produced by internal oxidation. Finally, the alloys undergo mostly internal rather than external oxidation in spite of their large Nb cotent, especially for the systems containing 30 wt% Nb. All these aspects appear to be related to the small solubility of niobium in the base metals and to the presence of intermetallic phases.

ACKNOWLEDGMENTS

The partial financial support from the European Community through research Contract CI1*-CT90-0859 and by the Italian MURST 40 and 60% is gratefully acknowledged.

References

1. M. C. Rebello, Y. Niu, F. Rizzo, and F. Gesmundo, *Oxid. Met.* **43**, 561 (1995).
2. M. J. Monteiro, Y. Niu, F. Rizzo, and F. Gesmundo, *Oxid. Met.* **43**, 527 (1995).
3. J. F. Oliveira, Y. Niu, F. Rizzo, and F. Gesmundo, *Oxid. Met.* **44**, 399 (1995).
4. Y. Niu, F. Gesmundo, and F. Viani, *Corros. Sci.* **36**, 1885 (1994).
5. Y. Niu, F. Gesmundo, and F. Viani, *Corros. Sci.* **36**, 1973 (1994).
6. Y. Niu, F. Gesmundo, and F. Viani, *Corros. Sci.* **37**, 169 (1995).
7. C. H. P. Lupis, *Chemical Thermodynamic of Materials* (North-Holland, New York, 1983), Ch. VII.
8. R. S. Roth, J. R. Dennis, and H. F. McMurdie, *Phase Diagrams for Ceramists* (The American Ceramic Society, Westerville, 1987), Vol. VI.
9. O. Kubaschewski, *High Temp.-High Press.* **4**, 1 (1972).
10. T. B. Massalski, J. L. Murry, L. H. Bennett and H. Baker (Eds.), *Binary Alloy Phase Diagrams*, (ASM, Metals Park, OH, 1986).
11. C. Wagner, *Z. Elektrochem.* **63**, 772 (1959).
12. R. A. Rapp, *Corrosion* **21**, 382 (1965).
13. F. Gesmundo, F. Viani, and Y. Niu, *Oxid. Met.* **42**, 409 (1994).
14. F. Gesmundo, Y. Niu, and F. Viani, *Oxid. Met.* **43**, 379 (1995).
15. F. Gesmundo, F. Viani, and Y. Niu, *Oxid. Met.* **45**, 51 (1996).
16. R. A. Rapp, *Acta Met.* **9**, 730 (1961).
17. P. Kofstad, *High Temperature Corrosion* (Elsevier Applied Science, New York, 1988).
18. J. Crank, *The Mathematics of Diffusion*, 2nd ed. (Oxford University Press, New York, 1975).
19. F. Gesmundo, F. Viani, Y. Niu, and D. L. Douglass, *Oxid. Met.* **42**, 239 (1994).
20. J. Takada, S. Yamamoto, S. Kikuchi and M. Adachi, *Oxid. Met.* **25**, 93 (1986).
21. P. J. Grundy and P. J. Nolan, *J. Mater. Sci. Lett.* **7**, 1086 (1972).
22. U. Seybolt and C. H. Mathewson, *Trans. Met. Soc. AIME* **117**, 156 (1935).
23. J. W. Park and C. J. Altstetter, *Met. Trans* **18A**, 43 (1987).
24. F. H. Stott and G. C. Wood, *Mater. Sci. Technol.* **4**, 1072 (1988).
25. H. A. Ahmed and W. W. Smeltzer, *J. Electrochem. Soc.* **133**, 212 (1986).
26. P. C. Patnaik and W. W. Smeltzer, *J. Electrochem. Soc.* **132**, 1226 (1985).
27. D. P. Whittle, Y. Shida, G. C. Wood, F. H. Stott, and B. D. Bastow, *Phil. Mag.* **A46**, 931 (1982).
28. A. Atkinson, *Mater. Sci. Technol.* **4**, 1046 (1988).
29. S. Guruswamy, S. M. Park, J. P. Hirth, and R. A. Rapp, *Oxid. Met.* **26**, 77 (1986).
30. L. S. Darken, *Trans. Am. Soc. Met.* **54**, 600 (1961).
31. L. Charrin, A. Combe, and J. Cabane, *Oxid. Met.* **37**, 65 (1992).
32. J. Takada, Y. Tomii, N. Yoshida, M. Sasaki, and M. Koiwa, *Oxid. Met.* **37**, 13 (1992).
33. L. Charrin, A. Combe, F. Cabane, and J. Cabane, *Oxid. Met.* **40**, 483 (1993).